

## Study of the Interaction Between *Apis mellifera* Venom and Micro-Heterogeneous Systems

Ana Paula Romani · Cássia Alessandra Marquezin · Ademilson Espencer Egea Soares · Amando Siuiti Ito

Received: 1 November 2005 / Accepted: 23 January 2006 / Published online: 16 May 2006  
© Springer Science+Business Media, Inc. 2006

The bee venom, used in treatment of inflammatory and articular diseases, is a complex mixture of peptides and enzymes and the presence of tryptophan allows the investigation by fluorescence techniques. Steady state and time-resolved fluorescence spectroscopy were used to study the interaction between bee venom extracted from *Apis mellifera* and three micro heterogeneous systems: sodium dodecylsulphate (SDS) micelles, sodium dodecylsulphate-poly(ethylene oxide) (SDS-PEO) aggregates, and the polymeric micelles LUTROL<sup>®</sup> F127, formed by poly(ethylene oxide)-poly(propylene oxide)- poly(ethylene oxide). Fluorescence parameters in buffer solution were typical of peptides containing tryptophan exposed to the aqueous medium, and they gradually changed upon the addition of surfactant and polymeric micelles, demonstrating the interaction of the peptides with the micro heterogeneous systems. Quenching experiments were carried out using the *N*-alkylpyridinium ions (ethyl, hexyl, and dodecyl) as quenchers. In buffer solution the quenching has low efficiency and is independent of the alkyl chain length of the quencher. In the presence of the micro heterogeneous systems the extent of static and dynamic quenching enhanced, showing that both fluorophore and quenchers reside in the microvolume of the aggregates. The more hydrophobic quencher (dodecyl pyridinium ion) provides higher values for  $K_{SV}$  and dynamic quenching

constants, and SDS-PEO aggregates are most efficient to promote interaction between peptides and alkyl pyridinium ions. The results proved that bee venom interacts with drug delivery micelles of the copolymer LUTROL<sup>®</sup> F127.

**Keywords** Bee venom · Melittin · Tryptophan · Micelle · Polymer

### Introduction

Bee venom contains a variety of different peptides, including melittin, apamin, adolapin, and mast cell degranulating peptide. The antiinflammatory properties and the anti arthritic effects of bee venom were demonstrated, and its potency in the inhibition of the inflammatory response was similar to that found for melittin, suggesting that this peptide is the main responsible for the pharmacological effects of the venom [1].

Melittin, the major toxic component in the venom of the honey bee, *Apis mellifera*, is a linear peptide composed of 26 amino acid residues and has a powerful hemolytic activity. It is a cationic peptide in which the amino terminal is composed of hydrophobic amino acids (residues 1–20), whereas the carboxy terminal end has a stretch of hydrophilic amino acids (residues 21–26), which give an amphiphilic character. Melittin is intrinsically fluorescent due to the presence of a tryptophan (Trp) residue, Trp-19, which is a sensitive probe to study the interaction of peptide with membranes and membrane-mimetic systems [2]. The importance of the membrane-bound form also stems from the observation that the amphiphilic  $\alpha$ -helical conformation of this hemolytic toxin in membranes resembles those of signal peptides, and of the envelope glycoprotein gp41 from the human immunodeficiency virus (HIV) [3]. A melittin-based recombinant

A. P. Romani · C. A. Marquezin · A. S. Ito (✉)  
Departamento de Física e Matemática, Faculdade de Filosofia,  
Ciências e Letras de Ribeirão Preto, Universidade de São Paulo,  
Ribeirão Preto, Brazil  
e-mail: amandosi@ffclrp.usp.br

A. E. E. Soares  
Departamento de Genética da Faculdade de Medicina de Ribeirão  
Preto, Universidade de São Paulo,  
Ribeirão Preto, Brazil

immunotoxin exhibited specific cytotoxicity against human tumor cells and the anticancer activity of melittin conjugated to a polymer was recently studied [4].

Micelles made of surfactant molecules have been used as simplified membrane model to investigate membrane proteins and peptides [5]. The study of micro-heterogeneous systems made of water-soluble polymers and surfactants in aqueous solution also has biological and technological implications [6]. According to the so-called “necklace model,” the structure of polymer-surfactant aggregates consists of spherical micelle beads, surrounded by polymer chains and connected by polymer strands [6]. Furthermore, also polymeric micelles have been studied extensively due to their applications in medicine, diagnostic imaging, environment sciences, and in drug delivery. They are usually composed of a hydrophobic core and a hydrophilic corona which acts as a steric stabilizer for the hydrophobic region in the aqueous environment. There are particular interest in self-assembled micelles with poly(ethylene oxide) (PEO) as the corona-forming block because of its excellent biocompatibility, long blood circulation time, and nontoxicity [7]. In that context, micelles from the triblock copolymer LUTROL® F127, formed by poly(ethylene oxide)-poly(propylene oxide)-poly(ethylene oxide), where the poly(propylene oxide) acts as the hydrophobic core, and the poly(ethylene oxide) as the hydrophilic corona, has been investigated for drug delivery [7].

In the present paper, we report results showing that fluorescence methods can be employed to study of the interaction between bee venom and three micro heterogeneous systems: SDS micelles, SDS-PEO aggregates and LUTROL® F127 polymeric micelles, in phosphate buffer solution (PBS). Intrinsic properties of tryptophan residue, component of melittin present in bee venom, were analyzed in aqueous medium containing the micro-heterogeneous systems, in combination with results of steady-state and time-resolved fluorescence quenching promoted by alkyl pyridinium ions. The pyridinium moiety constitutes an efficient quencher of Trp fluorescence, and it was observed a decrease in the emission of Trp residues in BSA and in small peptides due to the association of alkylpyridinium ions to the protein [8]. We performed experiments with alkyl pyridinium halides, which constitute a family of cationic surfactants employed to study also surfactant/protein association, due to the hydrophobicity of the alkyl chain [9].

## Materials and methods

Honey-bee workers were captured and immediately stored at  $-15^{\circ}\text{C}$  until dissection. Venom sacs were removed and the venom was collected in a capillary tube. Stock solution from bee venom was prepared in Milli-Q water.

LUTROL® F127 micelles were prepared by weighing out the appropriate quantity to the concentration of 2% and phosphate buffer was added under stirring and heating until the complete dissolution of copolymer. The sample remained in rest overnight before use. Sodium dodecyl sulphate (99%, Sigma, St. Louis) was purified by recrystallization from ethanol. Poly(ethylene oxide) (PEO, average molecular weight 8000 g/mol-Aldrich) and LUTROL® F127 (BASF) were used as received. The fluorescence quenchers *N*-Ethylpyridinium (NEP<sup>+</sup>) and *N*-Hexylpyridinium (NHP<sup>+</sup>) chlorides were prepared as described previously [10]. *N*-Dodecylpyridinium chloride (NDP<sup>+</sup>) was purchased from Aldrich and recrystallized from acetone.

Absorption spectra were registered on a Hitachi U-3000 spectrophotometer. Tryptophan fluorescence measurements and titration curves were performed on a Hitachi F4500 spectrofluorimeter. The anisotropy experiments in the steady state were made in a Hitachi F-3010 spectrofluorimeter equipped with polarizer filters.

Fluorescence decays and time-resolved anisotropy were measured using an apparatus based on the time-correlated single photon counting method. The excitation source was a Tsunami 3950 Spectra Physics titanium-sapphire laser, pumped by a Millennia X Spectra Physics solid state laser. The repetition rate of the pulses was set to 4.0 MHz using 3980 Spectra Physics pulse picker. The laser was tuned that a third harmonic generator BBO crystal (GWN-23PL Spectra Physics) gave the 296 nm excitation pulses that were directed to an Edinburgh FL900 spectrometer. The spectrometer was set in L-format configuration, the emission wavelength was selected by a monochromator, and emitted photons were detected by a refrigerated Hamamatsu R3809U microchannel plate photomultiplier. Soleil-Babinet compensator in the excitation beam and Glann-Thomson polarizer in the emission beam were used in anisotropy experiments. The FWHM of the instrument response function was typically 100 ps and time resolution was 12 ps per channel. A software provided by Edinburgh Instruments was used to analyze the individual decays, which were fitted to multiexponential curves:

$$I(t) = \sum \alpha_i e^{(-t/\tau_i)} \quad (1)$$

where  $\alpha_i$  and  $\tau_i$  are preexponential factor and lifetime of the component  $i$  of decay. The quality of the fit was judged by the analysis of the statistical parameter reduced- $\chi^2$  and by inspection of the residuals distribution. Mean lifetimes were calculated from intensity weighted lifetimes according to:

$$\langle \tau \rangle = \frac{\sum \alpha_i \tau_i^2}{\sum \alpha_i \tau_i} \quad (2)$$

In the fluorescence measurements, aliquots of venom extract stock solution (4% w/v) were added to volumetric flasks

containing buffer phosphate solution (PBS) pH 7.4 (0.01 M). In titration experiments, SDS and polymers were gradually added to the suspension. In quenching experiments, the following concentrations were used: SDS (0.05 M), SDS (0.05 M)-PEO (2%), and LUTROL F127 (2%). Using the reported value of  $5570 \text{ (M/cm)}^{-1}$  for the extinction coefficient of Trp in melittin [5], the estimated concentrations of peptide were:  $1.1 \times 10^{-5} \text{ M}$  in PBS,  $3.9 \times 10^{-5} \text{ M}$  in SDS,  $2.6 \times 10^{-5} \text{ M}$  in SDS-PEO, and  $1.6 \times 10^{-5} \text{ M}$  in LUTROL<sup>®</sup>. All solutions were stirred for 40 min. The concentration of *N*-alkylpyridinium ions was calculated based on the absorption measurements ( $\lambda_{\text{max}}$  258 nm). Aliquots of concentrated solutions of the quenchers (0.15 M) were added directly to the cuvette via a calibrated Hamilton microsyringe, and the emission intensities or probe fluorescence decay were registered after each addition. All measurements were performed at 293 K.

Dynamic light scattering measurements of micro-heterogeneous systems {SDS (0.05 M), SDS (0.05 M)-PEO (2%), and LUTROL<sup>®</sup> F127 (2%)} were carried out using a Brookhaven apparatus equipped with a Nd-YAG laser (532 nm). The temperature was kept at 25 °C and the measurements were made at a 90° angle. The data were analyzed using the software of the instrument.

## Results and discussion

### Dynamic light scattering

Dynamic light scattering measurements were made for the micro heterogeneous systems and provided mean values of effective diameter and polydispersity (Table 1). The value found for the diameter of SDS micelles was 6.9 nm and is greater than found in aqueous medium [11]. This enhancement is due the presence of buffer phosphate, which decrease the critical micellar concentration and favors the formation of larger micelles [12].

The diameter of SDS-PEO aggregates is greater than of SDS micelles (Table 1), result in agreement with the necklace model, according to which the radius and aggregation number of SDS micelles adsorbed on PEO chain are smaller than the values for free SDS micelles in water [11]. The hydrodynamic volume of the chain increases after addition of SDS, due to its behavior as a polyelectrolyte [13].

**Table 1** Data from dynamic light scattering on micro-heterogeneous systems

System	Diameter (nm)	Polydispersity
SDS (0.05 M)	6.9	0.131
SDS (0.05 M)-PEG (2%)	26.9	0.173
LUTROL <sup>®</sup> F127 (2%)	16.8	0.053

LUTROL<sup>®</sup> F127 micelles presents smaller diameter compared to SDS-PEO. Its size ( $16.8^{-1} \text{ nm}$ ) is considered desirable for drug-delivery [14] and is near to the previously reported value for the hydrodynamic radius (10.2 nm) calculated from diffusion data, with aggregation number 3, at 35 °C [15]. This system has low polydispersity, which is important to ensure the same number of probe molecules per micelle.

### Fluorescence of venom extract

As usually found in peptides containing tryptophan side chain exposed to water, the emission spectra of bee venom extract in buffer solution, pH 7.4, showed a broad band centered at 350 nm. The decay profile was fitted to a triexponential curve and a mean intensity weighted lifetime of 3.60 ns was obtained. Measured steady state anisotropy value was 0.024 and the time-resolved anisotropy decay was fitted to a two-component exponential curve, with rotational correlation times of 0.064 ns and 1.09 ns, which were related to the local Trp movement and overall motion of the whole peptide, respectively. This set of values is in agreement with values reported for Trp in melittin [5] or in peptides like melanocyte stimulating hormones and derivatives [16,17].

In the presence of micelles and polymeric micelles, fluorescence parameters were modified: the emission was blue shifted, the steady state anisotropy significantly increased and rotational correlation times also changed to higher values (Table 2). The spectral displacement is due to a decrease in the polarity around Trp residue, indicating that the fluorophore has moved to a hydrophobic region in the micelles. The increase in steady state anisotropy reflects the restriction that the circumventing molecules of surfactant and polymer impose to the movement of the fluorophore. The restriction to the rotational diffusion of the fluorophore is confirmed by the increase in the rotational correlation times obtained from the time-resolved anisotropy decay curves, as illustrated in Fig. 1 for bee venom in LUTROL<sup>®</sup> micelles. Data presented in Table 2 show that both rotation of Trp side chain (short correlation time) and overall tumbling of the peptide (long correlation time) are restricted in the micro-heterogeneous systems.

Lifetimes are also indicative of the occurrence of interaction between bee venom and micro heterogeneous systems. The presence of three lifetime components for Trp in peptides has been attributed to the occurrence of different rotational conformers of the indole ring around the  $C_{\alpha}$ - $C_{\beta}$  bond of the alanyl side chain and several recent studies support the rotamer model. Hellings *et al.* [18] stated in proteins an objective identification for lifetimes and corresponding rotamers. Clayton and Sawyer [19] showed that comparison with crystallographic data supported a correlation of Trp lifetimes with rotamer distributions. Pan and Barkley [20]

**Table 2** Fluorescence parameters of bee venom (4%): maximum emission wavelength ( $\lambda_{em}$ ), anisotropy ( $R$ ), rotational correlation time ( $\Phi_i$ ), and initial anisotropies ( $B_i$ )<sup>a</sup>

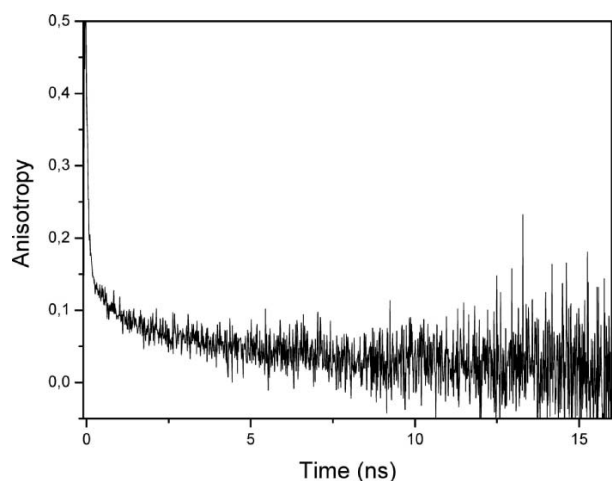
	$\lambda_{em}$	$R$	$\Phi_1$ (ns)	$\Phi_2$ (ns)	$B_1$	$B_2$
PBS (0.01 M)	350	0.024	1.09	0.064	0.139	0.235
SDS (0.05 M)	336	0.080	2.51	0.078	0.200	0.159
SDS (0.05 M)-PEO (2%)	335	0.078	2.21	0.085	0.149	0.230
LUTROL <sup>®</sup> F 127 (2%)	340	0.061	3.10	0.094	0.103	0.236

<sup>a</sup>Errors in rotational correlation times are 0.05 ns for  $\Phi_1$  and 0.005 ns for  $\Phi_2$ . Estimated errors in  $B_1$  and  $B_2$  amount to 10%.

studied multi exponential fluorescence emission in view of Trp side-chain  $\chi_1$  rotamer populations determined by <sup>1</sup>H-NMR. For many peptides the major lifetime component can be assigned to Trp  $g^-$  rotamer, with lifetimes ranging from 2.7 to 5.5 ns, and the less populated rotamer  $g^+$  is related to the short lifetime which has the smaller preexponential factor [20].

Theoretical calculations reported by Goldmann *et al.* [21] showed that in the Trp  $g^-$  rotamers the electron transfer process competes with fluorescence as a deactivation route for the excited state and the  $g^+$  rotamers present very high electron transfer rate, predominating over the fluorescence. It was shown that in Trp there is a pH-dependent interconversion between long and intermediate lifetimes reflecting interconversion between  $g^-$  and *trans* rotamers [22], and in melanocyte stimulating hormone the changes in parameters of fluorescence decay originate in the conformational changes driven by modifications in the ionization stated of titratable residues in the peptides [23].

The fluorescence decay of bee venom in buffer indicate predominance of *trans* and  $g^+$  rotamers, associated to the intermediate and short lifetimes. The multiexponential decay is also present in the presence of micro heterogeneous sys-

**Fig. 1** Time-resolved anisotropy of bee venom (4%) in LUTROL<sup>®</sup> F 127 micelles (2%) at 293 K

tems and we observed that mean lifetimes decreased in SDS micelles, as previously observed for melittin [5]. The main reason for the decrease in lifetime is the significant increase in the relative contribution of the short lifetime component ( $\alpha_3$  in Table 3), associated to  $g^+$  rotamer, with simultaneous decrease in the value of  $\alpha_1$ , associated to  $g^-$  rotamer. Thus, the result can be interpreted as consequence of conformational changes in the equilibrium between rotameric conformations of Trp, due to insertion in the micelles containing SDS. On the other hand, in the presence of LUTROL<sup>®</sup> micelles the lifetimes increased, but the preexponential factor of the long lifetime remained constant compared to the value in buffer. Despite of some interconversion between *trans* and  $g^+$  rotamers, the time resolved data suggests, in general terms, that the interaction with LUTROL<sup>®</sup> does not causes conformational changes in bee venom melittin.

#### Titration curves

In PBS solution, the maximum of absorption and emission of bee venom extracts were 284 and 350 nm, respectively. Several aliquots of a concentrated solution of SDS or SDS-PEO were added in PBS solution of bee venom and it was observed a concomitant increase in the fluorescence intensity. In the presence of aggregates the values of absorption and emission wavelengths were 278 and 335 nm respectively. The blue shift of the maximum emission wavelength suggests that Trp residue is located in a less polar environment [2] then, the probe may be associated with these aggregates.

Binding constants ( $K_b$ ) were determined using the relationship between the inverse of the variation of fluorescence emission intensity ( $\Delta F$ ) and the inverse of SDS concentration, according to [24]

$$\frac{1}{\Delta F} = \frac{1}{\Delta F_{max}} + \frac{1}{\Delta F_{max}} \frac{1}{K_b} \frac{1}{[SDS]} \quad (3)$$

**Table 3** Lifetime ( $\tau_i$ ) and preExponential factor ( $\alpha_i$ ) from multiexponential fit to decay profiles<sup>a</sup>

Medium	$\tau_1$ (ns)	$\tau_2$ (ns)	$\tau_3$ (ns)	$\alpha_1$	$\alpha_2$	$\alpha_3$	$\langle \tau \rangle$ (ns)
PBS	4.74	2.01	0.25	0.24	0.39	0.37	3.49
SDS	5.66	1.62	0.51	0.05	0.35	0.60	2.32
SDS-PEO	4.72	1.33	0.40	0.07	0.35	0.58	2.13
LUTROL <sup>®</sup>	5.54	2.32	0.50	0.23	0.55	0.22	3.80

<sup>a</sup>Excitation and emission wavelengths were 296 and 350 nm, respectively. Also shown weighted mean lifetime  $\langle \tau \rangle$ . Peptide concentration ranged between 1.1 and  $3.9 \times 10^{-5}$  M. Concentration of PBS was 0.01 M, SDS was 0.050 M, of PEO and LUTROL<sup>®</sup>, 2%. Deviations in lifetimes are 0.05 ns and in preexponential factors are 0.01.



where  $\Delta F = F - F_0$  is the difference between the fluorescence intensity at a certain concentration of SDS and the initial fluorescence intensity in the absence of surfactant, and  $\Delta F$  is related to the quantity of peptides associated with the aggregates. The straight line obtained in the plot of  $1/\Delta F$  as a function of  $1/[\text{SDS}]$ , may be employed to determine  $K_b$ . This constant was estimated considering the ratio between the intercept and the slope of the straight line.

The value of  $K_b$  is higher in SDS micelles ( $K_b = 381 \text{ M}^{-1}$ ) than is SDS/PEO aggregates ( $K_b = 180 \text{ M}^{-1}$ ) and the result can be interpreted based on the electrostatic effects influencing the interaction. The SDS micelles present negative surface potential due to the negative  $\text{SO}_3$  group, enhancing the concentration of the positively charged melittin near to the micelle surface. In the micro heterogeneous system containing PEO, this effect is reduced because the aggregates are made of clusters of SDS adsorbed on the PEO polymer chain [25]. The structure and composition of the surface region of the micelles is perturbed by the surrounding polymer [26], changing the surface potential and the access of the peptide to the micelles, decreasing the binding constant.

Similar titration was performed with LUTROL<sup>®</sup> polymeric micelles and the binding constant ( $K_b = 103 \text{ M}^{-1}$ ) was smaller than determined in the systems containing SDS. As the polymer is electrically neutral, the absence of electrostatic interaction with the peptide reduces the value of  $K_b$ .

Steady-state fluorescence quenching

The fluorescence quenching experiments were made in PBS solution, in SDS micelles, in SDS-PEO aggregates and in polymeric micelles of LUTROL<sup>®</sup> F 127. The fluorescence from bee venom was quenched by alkylpyridinium ions, as illustrated in Fig. 2 for *N*-dodecylpyridinium ion in LUTROL<sup>®</sup>. The Stern–Volmer constant ( $K_{SV}$ ) values were obtained from plots of  $F_0/F$  as a function of quencher concentration  $[Q]$ , where  $F_0$  and  $F$  are the fluorescence intensities in the absence and in the presence of the quencher:

$$F_0/F = 1 + K_{SV}[Q] \tag{4}$$

The plots are linear in the concentration range of quencher used, as shown in Fig. 3, and the quenching constants in the various systems are listed in Table 4. It is seen that in PBS solution the two short chain quenchers show approximately the same efficiency while the long chain ion ( $\text{NDP}^+$ ) presents higher  $K_{SV}$  value. The quenching is enhanced in the presence of aggregates which favour the contact between fluorophore and quencher. It was observed in melittin that Trp residue is located in the hydrophobic moiety between helical regions [27]. In this way, the presence of micelles favors the

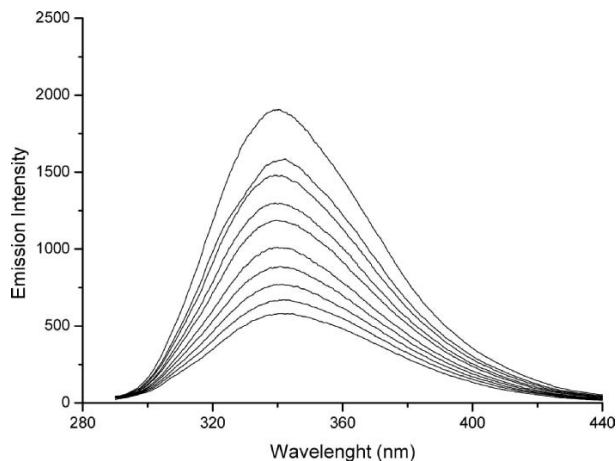


**Fig. 2** Fluorescence quenching of bee venom (4%) by *N*-dodecylpyridinium ion in LUTROL<sup>®</sup> F 127 micelles (2%) at 293 K. Intensity decreases with increase in the concentration of *N*-dodecylpyridinium. Excitation 296 nm

encounter of Trp with the pyridinium quencher bound to hydrophobic chains.

Higher  $K_{SV}$  values were obtained in SDS micelles and SDS-PEO aggregates due to the attractive electrostatic interaction between the negatively charged micellar surface and both positively charged residues in the peptide and pyridinium ion in the quencher. The SDS-PEO aggregates promote more efficient quenching, an effect probably related to the smaller aggregation number of this system compared to SDS micelles [28], which leads to increase the average number of quenchers per micelle, and facilitates the Trp-quencher encounter.  $K_{SV}$  values are reduced in polymeric micelles due the absence of electrostatic interaction between fluorophore, quencher ions, and micellar surface.

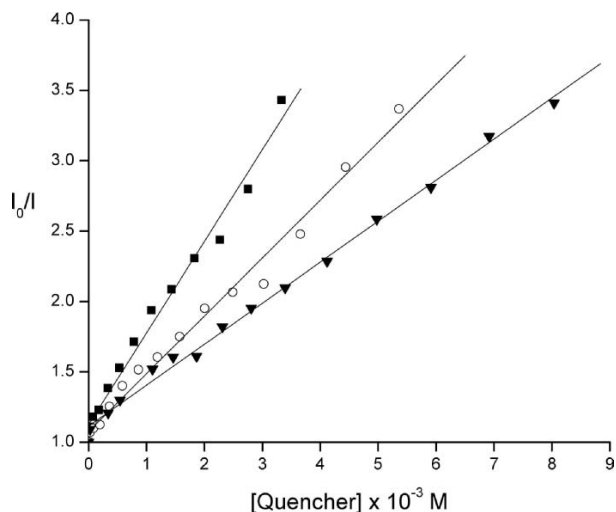


**Fig. 3** Stern–Volmer plot for fluorescence quenching of bee venom (4%) by *N*-alkylpyridinium ions (▼NEP<sup>+</sup>, ●NHP<sup>+</sup>, and ■NDP<sup>+</sup>) in SDS (0.05 M)-PEO (2%) aggregates at 293 K

**Table 4** Stern–volmer constants ( $K_{SV}$ ) for the fluorescence quenching of bee venom (4%) by alkyl pyridinium ions (NEP<sup>+</sup>, NHP<sup>+</sup>, and NDP<sup>+</sup>), in PBS and microheterogeneous systems

	$K_{SV}$ (M <sup>-1</sup> )		
	NEP <sup>+</sup>	NHP <sup>+</sup>	NDP <sup>+</sup>
PBS (0.01 M)	56 ± 1	56 ± 1	65 ± 1
SDS (0.05 M)	193 ± 11	323 ± 13	529 ± 34
SDS (0.05 M)-PEG (2%)	289 ± 10	436 ± 13	652 ± 24
LUTROL <sup>®</sup> F 127 (2%)	148 ± 3	289 ± 10	402 ± 33

$K_{SV}$  values are in agreement with reports on the literature [5], which shows that in SDS micelles, melittin tryptophan is less accessible to the aqueous medium, due to the partitioning of melittin into deeper regions of micelles. Data for NDP<sup>+</sup> suggest that Trp is in fact located in the hydrophobic interior of the aggregate, for the more effective quenching is promoted by the most hydrophobic quencher.

#### Dynamic quenching

The fluorescence decay profiles of bee venom were fitted to three-exponential curves whose lifetimes are related to the occurrence in several rotameric conformations, which have different extent of internal quenching. The alkylpyridinium ions increase the rate of nonradiative deactivation of bee venom fluorescence (Fig. 4) and the fitted data indicated that the three components are equally affected, maintaining the same relative contributions of their preexponential factors, as observed in absence of quencher. Thus, the addition of alkyl pyridinium ions does not affect the distribution of rotameric conformations of the peptide in the micelles.

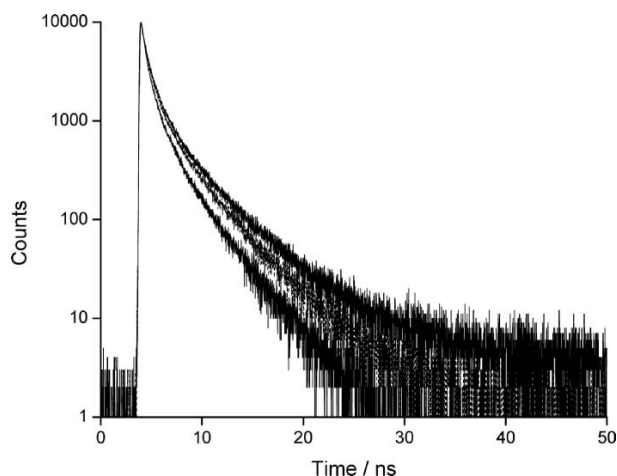


**Fig. 4** Fluorescence decay of bee venom (4%) in polymeric micelles of LUTROL<sup>®</sup> F127 (2%): quenching by *N*-dodecylpyridinium ion. Upper curve represents the decay without quencher and the other curves represent the decay in the presence of quencher (concentrations  $0.9 \times 10^{-3}$  M and  $3.2 \times 10^{-3}$  M)

Considering steady-state and time-resolved data, it can be observed that both static and dynamic quenching are present (Fig. 5). However static  $K_{SV}$  quenching constants are higher than  $K_D$  constants obtained from time-resolved measurements, showing that combined static and dynamic process are present, an observation which deserves future attention.

Although pyridinium charged quenchers may interact with the tryptophan residues in the surface of micelles, they may also quench buried tryptophan residues, depending on the size of the alkyl chain to which are bound [29]. The accessibility of Trp to the quenchers can be evaluated considering the collisional quenching constant ( $k_q$ ). The values of  $k_q$  were calculated from the relation  $K_D = k_q \tau_0$ , where  $K_D$  is the dynamic quenching constant, obtained from Stern–Volmer plots of the mean lifetimes, and  $\tau_0$  is the lifetime in absence of quencher. It was used the local concentration of quencher in the micelles and micro heterogeneous systems to determine  $k_q$ , a procedure that takes into account the volume of the aggregates instead of the volume of the bulk.

In PBS solution the values of  $k_q$  are in the order of  $0.5 \times 10^{10}$  M<sup>-1</sup> s<sup>-1</sup> (Table 5), which are consistent with the relatively high size of the peptide and the quenchers. The mobility of both, quencher and peptide, decreases in the presence of the aggregates and the bimolecular collisional constant decreases by a factor greater than 10. Quenchers with short chain (NEP<sup>+</sup> and NHP<sup>+</sup>) have higher mobility inside the aggregates, but the relatively immobile NDP<sup>+</sup> has the highest collisional constant in the three systems. This observation suggests that the hydrophobic region of the bee venom peptide penetrates into the polymeric micelle so that the proximity of tryptophan residue and pyridinium is facilitated.

Highest values of  $k_q$  occur in SDS-PEO aggregates, because it has the smaller aggregation number, and this fact

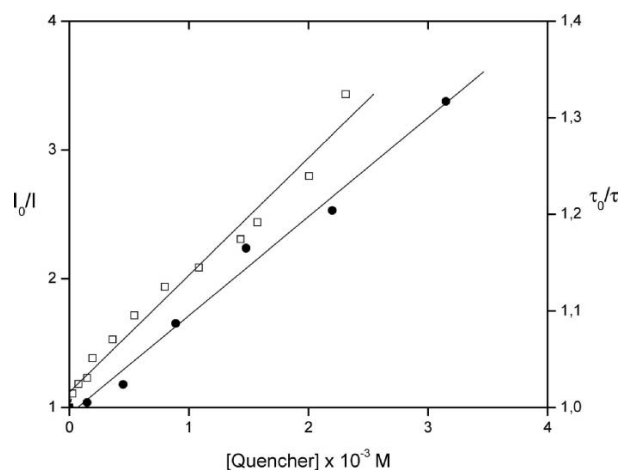


**Fig. 5** Steady-state (□) and time-resolved (●) data for Stern–Volmer plots of fluorescence quenching of bee venom (4%) by *N*-dodecylpyridinium ion in SDS (0.05 M)-PEO (2%) aggregates at 293 K

**Table 5** Bimolecular collisional rate constants ( $k_q$ ) for tryptophan and alkyl pyridinium ions.

	$k_q$ ( $10^8 \text{ M}^{-1} \text{ s}^{-1}$ )		
	NEP <sup>+</sup>	NHP <sup>+</sup>	NDP <sup>+</sup>
PBS (0.01 M)	43.9	55.3	69.5
SDS (0.05 M)	3.71	5.62	6.63
SDS (0.05 M)-PEO (2%)	3.84	7.78	9.53
LUTROL <sup>®</sup> F127 (2%)	1.21	0.84	2.75

increase the average number of quenchers per micelle. Polymeric LUTROL<sup>®</sup> micelle is a neutral system and presents the lowest  $k_q$  value, indicating that fluorescence properties of bee venom are consistent with the observations made in melittin, which has higher affinity for anionic membranes compared to neutral membranes [30].

#### Concluding remarks

Steady state and time-resolved fluorescence were useful techniques to study the interaction of bee venom with micro heterogeneous systems. The fluorescence properties of bee venom extracts are characteristic of melittin, the major component of the venom. The association with SDS micelles and SDS-PEO aggregates is mediated by hydrophobic effects and by electrostatic interactions between the negative head group of the surfactant and the positive amino acids residues in melittin. Due to the electrically neutral character of the copolymer, only hydrophobic effects drive the interaction of bee venom with LUTROL<sup>®</sup> F127 micelles.

Time-resolved measurements showed that the relative populations of lifetime components change in the presence of SDS containing aggregates, indicating conformational changes in the peptide when moving from the aqueous medium to the less polar environment of SDS containing micelles. Such effect is not present in the interaction with LUTROL<sup>®</sup>, showing that the polymeric micelles do not induce changes in peptide conformation. On the other hand, no modifications in the populations of lifetime components were promoted by addition of alkyl pyridinium ions, indicating that the presence of quencher does not affect the peptide conformation.

Bee venom melittin and alkyl pyridinium quencher have affinity for the aggregates, and the quenching process in SDS and in polymeric systems are more efficient than in buffer solution. The small size of SDS-PEO aggregates facilitates the encounter between quencher and Trp residue, enhancing the quenching of the fluorescence emission. In all cases, the long chain quencher NDP<sup>+</sup> is able to approach to a close contact with the Trp residue located in deep regions of the aggregates. The results as a whole demonstrated the affinity of the neutral copolymer LUTROL<sup>®</sup> F127 for the venom extract, without substantial changes in bee venom

melittin conformation, showing its potential as drug delivery system in pharmacological applications involving *apis mellifera* venom.

**Acknowledgements** This work was supported by grants from the Fundação de Amparo à Pesquisa do Estado de São Paulo (FAPESP—Proc. 03/05878-2) and Conselho Nacional de Desenvolvimento Científico e Tecnológico (CNPq), Brazil. The authors are pleased to thank Prof. Dr. Antonio Claudio Tedesco from Departamento de Química da Faculdade de Filosofia, Ciências e Letras de Ribeirão Preto, Universidade de São Paulo for the use of the spectrofluorometer Hitachi F4500 and Dr. Carla Cristina Schmitt Cavalheiro from Instituto de Química de São Carlos, Universidade de São Paulo, for the support in light scattering measurements.

#### References

- Park HJ, Lee SH, Son DJ, Oh KW, Kim KH, Song HS, Kim GJ, Oh GT, Yoon DY, Hong JT (2004) Antiarthritic effect of bee venom. *Arthr Rheum* 50(11):3504–3515
- Raghuraman H, Chattopadhyay A (2004) Interaction of melittin with membrane cholesterol: A fluorescence approach. *Biophys J* 87:2419–2432
- Raghuraman H, Chattopadhyay A (2005) Cholesterol inhibits the lytic activity of melittin in erythrocytes. *Chem Phys Lipids* 134:183–189
- Lavignac N, Lazenby M, Franchini J, Ferruti P, Duncan R (2005) Synthesis and preliminary evaluation of poly(amidoamine)-melittin conjugates as endosomolytic polymers and/or potential anticancer therapeutics. *Int J Pharm* 300:102–112
- Raghuraman H, Chattopadhyay A (2004) Effect of micellar charge on the conformation and dynamics of melittin. *Eur Biophys J* 33:611–622
- Sen S, Sukul D, Dutta P, Bhattacharyya K (2002) Solvation dynamics in aqueous polymer solution and in polymer-surfactant aggregate. *J Phys Chem B* 106:3763–3769
- Tang Y, Liu SY, Armes SP, Billingham NC (2003) Solubilization and controlled release of a hydrophobic drug using novel micelle-forming ABC triblock copolymers. *Biomacromolecules* 4:1636–1645
- Diaz X, Albuin E, Lissi E (2003) Quenching of BSA intrinsic fluorescence by alkylpyridinium cations. Its relationship to surfactant-protein association. *J Photochem Photobiol A: Chem* 155:157–162
- Weiss-López BE, González JV, Gamboa C (1996) Solubilization of *N*-alkylpyridinium ions in anionic nematic lyomesophases. *Langmuir* 12:4324–4328
- Romani AP, Vena FCB, Nassar PM, Tedesco AC, Bonilha JBS (2001) The binding of short chain *N*-alkylpyridinium ions to sodium dodecylsulfate micelles. *J Colloid Interface Sci* 243:463–468
- Dai S, Tam KC (2001) Isothermal titration calorimetry studies of binding interactions between polyethylene glycol and ionic surfactants. *J Phys Chem B* 105:10759–10763
- Nassar PM, Nogueira LC, Bonilha JBS (1995) Photophysical probe studies of polymer-detergent interactions. *J Braz Chem Soc* 6(2):173–178
- Dhara D, Shah DO (2001) Stability of sodium dodecyl sulfate micelles in the presence of a range of water-soluble polymers: A pressure-jump study. *J Phys Chem B* 105:7133–7138
- Van Domeselaar GH, Kwon GS, Andrew LC, Wishart DS (2003) Application of solid phase peptide synthesis to engineering

- PEO-peptide block copolymers for drug delivery. *Coll Surf B: Bioint* 30:323–334
15. Alexandridis P, Alan Hatton T (1995) Poly(ethylene oxide)-poly(propylene oxide)-poly(ethylene oxide) block copolymer surfactants in aqueous solution and at interfaces: Thermodynamics, structure, dynamics, and modeling. *Coll Surf A: Physicochem Eng Aspects* 96:1–46
  16. Ito AS, de L Castrucci AM, Hruby VJ, Hadley ME, Krajcarski DT, Szabo AG (1993) Structure activity correlations of melanotropic peptides in model lipids by tryptophan fluorescence studies. *Biochemistry* 32:12264–12272
  17. Ito AS, Souza ES, Barbosa SR, Nakaie CR (2001) Fluorescence study of conformational properties of melanotropins labeled with aminobenzoic acid. *Biophys J* 81:1180–1189
  18. Hellings M, De Maeyer M, Verheyden S, Hao Q, Van Damme EJM, Peumans WJ, Engelborghs Y (2003) The dead-end elimination method, tryptophan rotamers, and fluorescence lifetimes. *Biophys J* 85:1894–1902
  19. Clayton AHA, Sawyer WH (1999) Tryptophan rotamer distributions in amphipathic peptides at a lipid surface. *Biophys J* 76:3235–3242
  20. Pan C-P, Barkley MD (2004) Conformational effects on tryptophan fluorescence in cyclic hexapeptides. *Biophys J* 86:3828–2835
  21. Goldman C, Pascutti PG, Piquini P, Ito AS (1995) On the contribution of electron transfer reaction to the quenching of tryptophan fluorescence. *J Chem Phys* 103:10614–10620
  22. Marquezin CA, Hirata IY, Juliano L, Ito AS (2003) Tryptophan as a fluorescent probe for acid-base equilibrium. *Biopolymers* 71:569–576
  23. Fernandezm RM, Vieira RFF, Nakaye CR, Lamy MT, Ito AS (2005) Acid base titration of melanocortin peptides: Evidence of Trp rotational conformers interconversion. *Biopolymers* 80:643–650
  24. Tabak M, Borissevitch IE (1992) Interaction of dipyrindamole with micelles of lysophosphatidylcholine and with serum albumin: fluorescence studies. *Biochim Biophys Acta* 1116:241–249
  25. Dhara D, Shah DO (2001) Effect of poly(ethylene glycol)s on micellar stability of sodium dodecyl sulfate. *Langmuir* 17:7233–7236
  26. Sen S, Sukul D, Dutta P, Bhattacharyya K (2001) Fluorescence anisotropy decay in polymer-surfactant aggregates. *J Phys Chem A* 105(32):7495–7500
  27. Constantinescu I, Lafleur M (2004) Influence of the lipid composition on the kinetics of concerted insertion and folding of melittin in bilayers. *Biochim Biophys Acta* 1667:26–37
  28. Romani AP, Gehlen MH, Itri R (2005) Surfactant-polymer aggregates formed by sodium dodecyl sulfate, poly-*N*-vinyl-2-pyrrolidone and polyethyleneglycol. *Langmuir* 21:127–133
  29. Sultan NAM, Swamy MJ (2005) Fluorescence quenching and time-resolved fluorescence studies on *Trichosanthes dioica* seed lectin. *J Photochem Photobiol B: Biol* 80:93–100
  30. Lazaridis T (2005) Implicit solvent simulations of peptide interactions with anionic lipid membranes. *Proteins: Struct Funct Bioinf* 58:518–527